IEEE Access
Multidisciplinary ⋮ Rapid Review ⋮ Open Access Journal

Received 26 May 2023, accepted 16 June 2023, date of publication 21 June 2023, date of current version 28 June 2023.

Digital Object Identifier 10.1109/ACCESS.2023.3288124

RESEARCH ARTICLE

Robust Speed Controller Using Dual Adaptive Sliding Mode Control (DA-SMC) Method for PMSM Drives

HOANG NGOC TRAN[1] AND JAE WOOK JEON[2], (Senior Member, IEEE)
[1]Department of Software Engineering, FPT University, Can Tho 94000, Vietnam
[2]Department of Electrical and Computer Engineering, Sungkyunkwan University, Suwon 16419, South Korea

Corresponding author: Jae Wook Jeon (jwjeon@skku.edu)

This work was supported by Institute of Information and Communications Technology Planning and Evaluation (IITP) grant funded by the Korea government [MSIT(Ministry of Science and Information and Communication Technology)] (2021-0-01364, An intelligent system for 24/7 real-time traffic surveillance on edge devices).

ABSTRACT A robust mechanical parameter estimation together with adaptive speed control algorithms for permanent magnet synchronous motor (PMSM) drive systems based on the dual adaptive sliding-mode method is proposed in this paper. First, a robust adaptive sliding mode mechanical observer (RASM) and mechanical parameter identification (MPI) are proposed to eliminate system parameter errors in the first rotation. Based on RASM-MPI, the correct mechanical parameters are estimated from the system disturbance value. Then, an adaptive sliding-mode speed control (ASMSC) is applied to reduce the chattering inherent in the control signal and improve the convergence time to reach the sliding-mode surface. From the second rotation, the RASM identifies unknown external load torque and provides feed-forward compensation for the ASMSC to improve the speed control of the PMSM. All the proposed methods are applied to an industrial motor drive. The experimental results verified that the proposed scheme can estimate system parameters accurately within a short time. In addition, the speed controller can run stably, and with less error.

INDEX TERMS PMSM drives, adaptive sliding-mode control (ASMC), integral sliding mode (ISMC), parameter identification, sliding-mode observer (SMO).

I. INTRODUCTION

PMSMs are now widely used in many industrial applications that include robotics, electric vehicles, industrial drives, and machine tools, due to their simple structure, high precision, high efficiency, high reliability, and excellent torque control performance [1], [2]. In a PMSM controller, parameter accuracy is an essential component that impacts the whole system's control precision. To achieve the high dynamic performance of the speed control, it is necessary to consider the mechanical characteristics, such as the rotational inertia, the viscous friction coefficient, and the load torque. If these parameters can be accurately estimated, the adaptive controllers of PMSM systems can easily achieve high accuracy.

Many parameter estimation methods have been studied and developed to improve accuracy. References [3], [4], [5], and [6] present a model reference adaptive system (MRAS) that is simple, and easy to implement. However, real-time load torque estimation is not achievable with this estimated method. The parameter adaptation method is used to estimate the parameters by using the adaptive law or cost function, such as recursive Least Squares (rLS) [3], [4], and extended Kalman filter (EKF) [5], [6]. However, these methods are complex and difficult to apply to real systems. The rLS method requires a long estimation time and a lot of data, so when applied in practice, it has many limitations [7].

In recent years, the disturbance load torque observer (DLTO) and sliding-mode observer (SMO) are two commonly used methods to estimate the parameters for PMSM. References [8], [9], [10], and [11] apply the DLTO method to estimate viscous friction, rotational inertia, and load torque.

The associate editor coordinating the review of this manuscript and approving it for publication was Jinquan Xu.

Although they are capable of achieving the estimated performance, the accuracy and stability of the DLTO methods are low. Meanwhile, the SMO method offers attractive advantages in terms of noise immunity and minimal sensitivity to parameter fluctuations of the whole system compared with DLTO technique. Several SMO approaches have been proposed to estimate the parameters. References [11] and [12] design an SMO to improve the influence of noise on the estimated coefficients' accuracy. However, the quality improvement is slight. In addition, a second-order SMO is proposed to estimate the mechanical system [13], [14]. In this case, a low-pass filter (LPF) must be used to obtain the results, which will cause amplitude attenuation and a phase lag.

In addition to the accuracy of the mechanical parameter identification, the accuracy and stable operation of the speed controller are important in the PMSM system. Many methods have been proposed, including traditional methods and intelligent control methods, such as the PID control method [15], [16], [17], fuzzy logic control [18], [19], model predictive control [20], [21], and artificial neural network control [22], [23]. Traditional PID control methods cannot respond quickly limiting external noises and parameter changes to maintain good operation for the motor's actual speed. Meanwhile, intelligent methods cannot be applied to systems with limited hardware. The complexity, as well as the large amount of computation involved, are barriers to applying these intelligent methods in practical systems. Among them, the sliding-mode control (SMC) stands out as a method that can be applied simply, and with high accuracy and stability [24], [25], [26], [27], [28], [29]. However, the frequent switching of the system structure in SMC, which has grown to be a significant element impacting the control, makes chattering of the system inevitable. As a result, enhancing SMC deployment through chatter reduction has emerged as a major study area.

This paper proposes an effective method to improve the accuracy and performance of the mechanical parameter identification and the speed controller of the PMSM. The proposed method can reduce the influence of noise on the estimated parameters by reducing the chattering and reaching time to reach the sliding-mode surface. The parameters without error are provided feed-forward compensation for the ASMSC to reduce the overshoot when there is a reference speed jump. The experiments are performed with an industrial motor driver. The proposed methods are compared with existing conventional methods to verify their effectiveness and practical applicability. Fig. 1 shows the proposed structure of the PMSM system via the DA-SMC approach. The contributions of this paper are outlined as follows:

1) A robust observer and mechanical parameter identification (RASM-MPI) scheme is developed; this contains a global integral sliding mode observer using the adaptive reaching law, and a parameters identification approach. With the proposed method, the parameters are estimated with high accuracy. The external load torque is tracked and it is used to achieve forward compensation of sudden load torque for the speed controller loop in real time.
2) An adaptive sliding mode speed controller (ASMSC) is proposed to improve the dynamic performance of the PMSM speed regulation system including reducing the effect of disturbance and overshooting. An improved reaching law and sliding surface are applied to reduce chattering and reaching time.

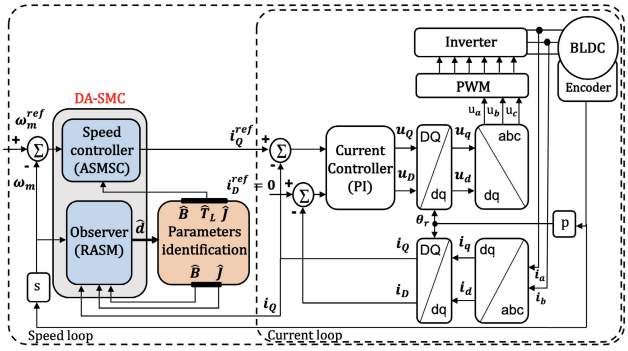

FIGURE 1. Control structure of the PMSM system via the DA-SMC approach.

The remainder of this paper is organized as follows. Section II introduces the mathematical model of the PMSM, while Section III describes the RASM-MPI. Section IV details the proposed adaptive sliding mode speed controller for the speed loop, then Section V describes the simulation and experimental results. Section VI concludes the paper.

II. MATHEMATICAL MODELING OF A PMSM

The dynamics of a PMSM in the rotor d-q coordinates can be expressed as follows [30], [31], [32], [33]:

$$\begin{bmatrix} u_Q \\ u_D \end{bmatrix} = \begin{bmatrix} R + sL_q & \omega_r L_d \\ -\omega_r L_q & R + sL_d \end{bmatrix} \begin{bmatrix} i_Q \\ i_D \end{bmatrix} + \begin{bmatrix} \omega_r \Phi_m \\ 0 \end{bmatrix} \quad (1)$$

$$T_e = 1.5p\left[\Phi_m i_Q + \left(L_d - L_q\right) i_Q i_D\right] \quad (2)$$

where u_Q, u_D are voltages; i_Q, i_D are current; L_q and L_d are inductances of the $q-$ and $d-axes$, respectively; R is the stator resistance; Φ_m is the flux linkage of permanent magnets; ω_r is the angular speed; T_e is the electrical magnetic torque; p is the number of pole pairs; and "s" represents the Laplace operator.

In this study, the linearized model is considered, so the d-axis current is set to zero. The electrical magnetic torque can be expressed as follows:

$$T_e = K_t i_Q = J\dot{\omega}_m + B\omega_m + T_L \quad (3)$$

where K_t is the torque constant; J is the rotational inertia; B is the coefficient of viscous frictional; T_L is the load torque; and ω_m is the mechanical angular speed of rotor.

Based on (1) and (3), the parameters of the PMSM can be divided into two models of electrical (R, $L_{q,d}$, p, *and* Φ_m), and mechanical (J, B, *and* T_L) parameters. In particular, the electrical parameters can be easily identified by using sensors

TABLE 1. Fastech, Co., motor model K6LS30N2 parameters.

Parameter	Value
Resistance (R)	1.4Ω
Phase dq-axis inductance (L_d, L_q)	$1.13mH$
Viscous friction (B_n)	$1.2 \times 10^{-3} N.m.s/rad$
Moment of total inertia (J_n)	$68.58 \times 10^{-6} kg.m^2$
Number of pole pairs (p)	5
Load torque (T_L)	$6.12 \times 10^{-2} N.m/A$

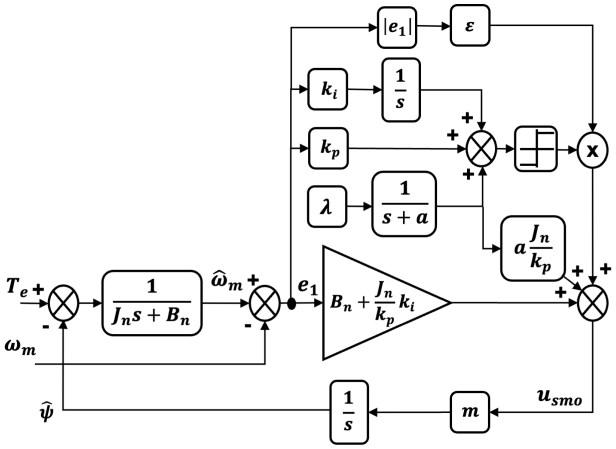

FIGURE 2. Schematic block diagram of the RASM observer.

or instruments. However, the identified mechanical parameters, which include parameter errors and sudden load torque changes, are more complicated. These parameters need to be accurately identified because they are important in the design of a speed controller for a PMSM system. Therefore, this paper designed the RASM-MPI to improve the accuracy of the estimated mechanical parameters (J, B, *and* T_L).

III. ROBUST ADAPTIVE SLIDING MODE MECHANICAL PARAMETER IDENTIFICATION

A. ROBUST ADAPTIVE SLIDING MODE OBSERVER

The RASM-MPI consists of the Adaptive Sliding Mode Observer (ASMO) and Mechanical Parameter Identification. The purpose of the sliding mode observer is to track the lumped disturbance, an unknown factor that results in an unexpected change in speed. By using parameter identification to monitor the lumped disturbance, the actual coefficients can be accurately determined. The dynamic equation of the motor, incorporating the impact of lumped disturbances, can be represented as follows:

$$\begin{aligned} T_e &= (J_n + \Delta J)\,\dot{\omega}_m + (B_n + \Delta B)\omega_m + T_L \\ &= J_n\dot{\omega}_m + B_n\omega_m + \psi \end{aligned} \tag{4}$$

where $J_r = J_n + \Delta J$, and $B_r = B_n + \Delta B$. J_r and B_r are the real inertia and the real viscous friction of the system. J_n and B_n are nominal parameters; ΔJ and ΔB are parameter errors between the real system and the nominal value; and $\psi = \Delta J\dot{\omega}_m + \Delta B\omega_m + T_L$ represents the disturbances including parameter error and load torque.

The equation of the dynamic model is rewritten as follows:

$$\begin{cases} \dot{\omega}_m = \dfrac{1}{J_n}\left(T_e - B_n\omega_m - \psi\right) \\ \dot{\psi} = v_r \end{cases} \tag{5}$$

where $v_r = \Delta J\ddot{\omega}_m + \Delta B.\dot{\omega}_m + \dot{T}_L$ represents the rate of change in system disturbances ψ.

The design of the RASM observer can be formulated for the objective of parameters estimation as follows:

$$\begin{cases} \dot{\hat{\omega}}_m = \dfrac{1}{J_n}\left(T_e - B_n\hat{\omega}_m - \hat{\psi} + u_{smo}\right) \\ \dot{\hat{\psi}} = mu_{smo} \end{cases} \tag{6}$$

where $\hat{\omega}_m$ is the estimated value of speed ω_m, $\hat{\psi}$ is the estimated value of disturbances ψ, m is a sliding-mode parameter that will be explored in more detail in the upcoming section, and u_{smo} denotes the sliding mode control function.

The variables are defined as $e_1 = \hat{\omega}_m - \omega_m$, $\dot{e_1} = \dot{\hat{\omega}}_m - \dot{\omega}_m$, and $e_2 = \hat{\psi} - \psi$. In this paper, the integral sliding surface is used as a solution to improve the accuracy and lower the steady-state error in the system. This approach, which involves the use of integral action, enhances the system's immunity to interference by compensating for any uncertainty in the model. Furthermore, by placing the initial stages of sliding mode motion within the control range through global sliding, the occurrence of the undesirable chattering phenomenon is reduced. The sliding surface for this method can be formulated as follows:

$$S = k_p e_1 + k_i \int_0^t e_1 dt + H(t) \tag{7}$$

where k_p, k_i are positive coefficients that allow for customization in the design of the sliding surface, and $k_p, k_i \epsilon R^+$ and $S \epsilon R$. The control input, $H(t)$, plays a crucial role in ensuring the global sliding mode is established. To ensure the sliding mode control remains within the reachable range at all times, $H(t)$ must possess three specific properties, as described below:

1) At the starting point of time, $t = 0$, the value of $H(0) = -\left(k_p e_1(0) + k_i \int_0^0 e_1(\tau)d\tau\right)$;
2) At the time $t \to \infty$, the value of $H(t) \to 0$;
3) The derivative of the control input, $H(t)$, must exist.

According to the three conditions listed above, the control input $H(t)$ is designed as $H(t) = \lambda e^{-at}$ where a is a positive constant. Combining with Eq. (7) results in the expression for the global integral sliding surface, which is $S = k_p e_1 + k_i \int_0^t e_1 dt + \lambda e^{-at}$. The value of λ can be found by solving for it using condition 1, which gives $\lambda = -k_p e_1(0)$. The speed of the approach towards the sliding mode is determined by the variable speed approach law. The adaptive reaching law is used in this approach as follows:

$$\dot{S} = \varepsilon\,|e_1|\,sgn(S) \tag{8}$$

where ε is a parameter that determines the switching gain. If the value of ε is too high, this can result in excessive

chattering within the system, whereas if it is too low, it can increase the response time of the system to external changes. The proposed RASM observer features an adaptive reaching law [34], which adjusts the bandwidth based on the state error $|e_1|$. As the state error decreases, the bandwidth of the observer also decreases, leading the system trajectory to reach the equilibrium point. This results in a reduction of chattering compared to the conventional reaching law $\dot{S} = \varepsilon sgn(S)$. Fig.2 shows a schematic block diagram of the RASM observer.

Once the system has entered the sliding mode, the rate of change of the sliding surface, $\dot{S} = 0$. If external disturbances occur, such as load torque or friction coefficient, the sliding mode will continue to maintain stability, with:

$$\begin{aligned} \dot{e_1} &= \dot{\hat{\omega}}_m - \dot{\omega_m} \\ &= \frac{1}{J_n}\left(B_n(\omega_m - \hat{\omega}_m) + (\psi - \hat{\psi}) + u_{smo}\right) \end{aligned} \tag{9}$$

then,

$$\begin{aligned} \dot{S} &= \frac{k_p}{J_n}\left(B_n(\omega_m - \hat{\omega}_m) + (\psi - \hat{\psi}) + u_{smo}\right) \\ &\quad + k_i(\hat{\omega}_m - \omega_m) - a\lambda e^{-at} \\ &= \left(k_i - k_p\frac{B_n}{J_n}\right)e_1 - \frac{k_p}{J_n}e_2 + \frac{k_p}{J_n}u_{smo} - a\lambda e^{-at} \end{aligned} \tag{10}$$

The function switching control law can be derived from the combination of (8) and (10) as:

$$u_{smo} = \left(B_n - \frac{J_n}{k_p}k_i\right)e_1 + e_2 + \frac{J_n}{k_p}a\lambda e^{-at} + \varepsilon\,|e_1|\,sgn(S) \tag{11}$$

A detailed analysis of the stability conditions for the RASM system has been conducted using the Lyapunov function $V(x) = s^2/2$, where x is the state vector. The results of the analysis show that if the system is stable, then the reachability condition below is satisfied:

$$\dot{V}(x) = S\dot{S} < 0 \tag{12}$$

Combining (8), (10), and (12) gives:

$$\begin{aligned} S\dot{S} &= S\left(\left(k_i - k_p\frac{B_n}{J_n}\right)e_1 - \frac{k_p}{J_n}e_2 + \frac{k_p}{J_n}u_{smo} - a\lambda e^{-at}\right) \\ &= S\varepsilon\,|e_1|\,sgn(S) \\ &= \varepsilon\,|e_1|\,|S| \end{aligned} \tag{13}$$

Thus, to ensure the stability of the system, it is only necessary that $\varepsilon < 0$ be satisfied, which results in $\dot{V}(x) = S\dot{S} < 0$.

It is evident that the error e_1 and its derivative $\dot{e}_1$ can reach zero in a finite amount of time during the sliding mode, resulting in $e_1 = \dot{e}_1 = 0$. As a result, the error equation (10) can be reduced to a more straightforward form as

$$\begin{cases} e_2 = u_{smo} - \dfrac{J_n}{k_p}a\lambda e^{-at} \overset{t\to\infty}{\rightarrow} e_2 = u_{smo} \\ \dot{e_2} = mu_{smo} - v_r \end{cases} \tag{14}$$

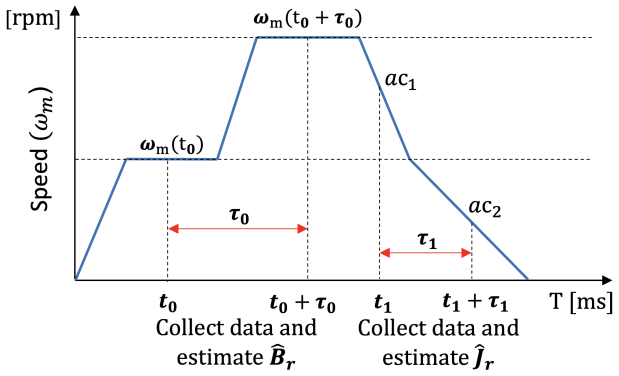

FIGURE 3. Speed waveform used to estimate the mechanical parameter of MPI.

which can also be expressed as

$$\dot{e}_2 - me_2 + v_r = 0 \tag{15}$$

Therefore, the solution for e_2 can be found as follows:

$$e_2 = e^{mt}\left(C - \int v_r e^{-mt}dt\right) \tag{16}$$

where C is a constant value. To ensure that the disturbance estimation error e_2 will converge to zero, the sliding-mode parameter must be negative ($m < 0$), and the rate at which e_2 approaches zero is proportional to m. Fig. 22 presents a schematic block diagram of the RASM observer:

B. MECHANICAL PARAMETERS IDENTIFICATION

As indicated by the analysis, the proposed RASM observer approach is capable of continuously monitoring real-time information regarding the lumped disturbance, including the mechanical parameters of the PMSM control system. Additionally, the method effectively suppresses the chattering phenomenon that is inherent in sliding mode. As a result, the mechanical parameters can be accurately extracted from the RASM observer.

Fig. 3 shows the speed waveform of the identification principle. The first rotation motor of the motor according to the reference speed waveform above is done to estimate the $\hat{B}_r$, $\hat{J}_r$ values. In Fig. 3, the estimation of the B stage from t_0 to $t_0 + \tau_0$ requires the operation of the motor at two different constant speeds. At this stage, both the feedback speed ω_m and the estimated disturbance $\hat{\psi}$ are utilized to estimate the parameter $\hat{B}_r$. After estimating the real viscous friction, the motor runs at two different constant deceleration rates from t_1 to $t_1 + \tau_1$. During this stage, the real inertia $\hat{J}_r$ is estimated based on the information on the deceleration ac, and the estimated disturbances $\hat{\psi}$. Finally, after determining the values of $\hat{B}_r$, and $\hat{J}_r$, the estimated parameter error must be updated to zero. Therefore, the estimated disturbance is now the estimated load torque (T_L), which can be used to compensate for the sudden load torque. This approach is applied to identify the parameters of the MPI, which are explained thoroughly in the subsequent section.

1) VISCOUS FRICTION IDENTIFICATION

The estimated real value of parameter B_r can be represented as $\hat{B}_r = B_n + \Delta\hat{B}$. Thus, it is possible to calculate the estimated parameter $\hat{B}_r$ by determining the error $\Delta\hat{B}$, since the nominal value of B_n is already known. During the estimation of B_r as depicted in Fig.3, the motor must run at two different constant speeds such that $\omega_m(t_0) \neq \omega_m(t_0 + \tau_0)$, and $\dot{\omega}_m(t_0) = \dot{\omega}_m(t_0 + \tau_0) = 0$. In Fig.3, the constant time delays τ_0 represent two different periods of time for the motor to operate at two different steady speeds. As the motor runs at the first steady speed $\omega_m(t_0)$, and the second steady speed $\omega_m(t+\tau_0)$, the disturbances can be estimated using the RASM observer as follows:

$$\hat{\psi}(t_0) = \Delta\hat{J}\dot{\omega}_m(t_0) + \Delta\hat{B}\omega_m(t_0) + T_L \tag{17}$$

$$\hat{\psi}(t_0 + \tau_0) = \Delta\hat{J}\dot{\omega}_m(t_0 + \tau_0) + \Delta\hat{B}\omega_m(t_0 + \tau_0) + T_L \tag{18}$$

When the motor has stabilized and reached a constant speed, $dot\omega_m$ can be considered as zero, and the load torque can be assumed to be constant as well. Subtracting (18) from (17), the result is obtained:

$$\hat{\psi}(t_0 + \tau_0) - \hat{\psi}(t_0) = \Delta\hat{B}\left(\omega_m(t_0 + \tau_0) - \omega_m(t_0)\right) \tag{19}$$

Thus, the estimate of the parameter error $\Delta\hat{B}$ can be estimated as follows:

$$\Delta\hat{B} = \frac{\hat{\psi}(t_0 + \tau_0) - \hat{\psi}(t_0)}{\omega_m(t_0 + \tau_0) - \omega_m(t_0)} \tag{20}$$

Hence, $\hat{B}_r$ can be determined as:

$$\hat{B}_r = B_n + \Delta\hat{B} = B_n + \frac{\hat{\psi}(t_0 + \tau_0) - \hat{\psi}(t_0)}{\omega_m(t_0 + \tau_0) - \omega_m(t_0)} \tag{21}$$

2) MOMENT OF TOTAL INERTIA IDENTIFICATION

After estimating the real viscous friction of the system (B_r), the nominal parameter B_n in (5) can be updated with $\hat{B}_r$. According to (17), the estimation of the disturbance, $\hat{\psi}$, at time t_1, and $t_1 + \tau_1$ can be expressed as:

$$\begin{cases} \hat{\psi}(t_1) = \Delta\hat{J}\dot{\omega}_m(t_1) + T_L \\ \hat{\psi}(t_1 + \tau_1) = \Delta\hat{J}\dot{\omega}_m(t_1 + \tau_1) + T_L \end{cases} \tag{22}$$

$$\Rightarrow \begin{cases} \hat{\psi}(t_1) = \Delta\hat{J}ac_1 + T_L \\ \hat{\psi}(t_1 + \tau_1) = \Delta\hat{J}ac_2 + T_L \end{cases} \tag{23}$$

The real inertia J_r is estimated based on the two different constant accelerations (ac_1 *and* ac_2) corresponding to two different periods of time (τ_1). Subtracting the two equations, the following result is obtained:

$$\hat{\psi}(t_1 + \tau_1) - \hat{\psi}(t_1) = \Delta\hat{J}\left(ac_2 - ac_1\right) \tag{24}$$

Then, $\Delta\hat{J}$ can be obtained as follows:

$$\Delta\hat{J} = \frac{\hat{\psi}(t_1 + \tau_1) - \hat{\psi}(t_1)}{ac_2 - ac_1} \tag{25}$$

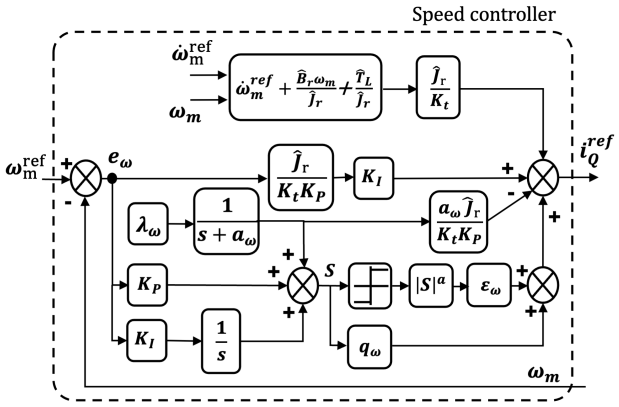

FIGURE 4. Schematic block diagram of the ASMSC controller.

Therefore, the estimated value of parameter $\hat{J}_r$ can be obtained using the following equation:

$$\hat{J}_r = J_n + \Delta\hat{J} = J_n + \frac{\hat{\psi}(t_1 + \tau_1) - \hat{\psi}(t_1)}{ac_2 - ac_1} \tag{26}$$

To perform optimally, the PMSM control system must have the ability to accurately and promptly estimate the load torque. Therefore, the load torque needs to be observed in real-time.

3) LOAD TORQUE IDENTIFICATION

By accurately estimating the parameters B_r and J_r, the nominal parameters B_n and J_n in (6) can be substituted with the estimated values, resulting in $\Delta J = J_r - \hat{J}_r = 0$ and $\Delta B = B_r - \hat{B}_r = 0$. The expression in (6) can then be rewritten as follows.

$$\begin{cases} \dot{\hat{\omega}}_m = \frac{1}{\hat{J}_r}\left(T_e - \hat{B}_r\hat{\omega}_m - \hat{\psi} + u_{smo}\right) \\ \dot{\hat{\psi}} = mu_{smo} \end{cases} \tag{27}$$

Finally, the revised disturbance estimation $\hat{\psi}$ can be presented as follows:

$$\hat{\psi} = T_L \tag{28}$$

The proposed method RASM-MPI, when implemented in the real system, has the capability to accurately estimate the actual values of B and J, thus enabling online observation of the load torque to counter any load disturbance and avoiding sudden changes in load torque. The lumped disturbance estimated from the RASM method will have higher accuracy than other traditional SMC methods. Thus, it makes the speed controller's operation better, reduces overshoot, and is more stable. The results will be compared in the experimental section.

IV. ADAPTIVE SLIDING-MODE SPEED CONTROLLER

After determining the values of B, J, and observing T_L, they are utilized to adjust the speed controller. In this paper, an adaptive sliding-mode speed controller (ASMSC) is introduced to enhance the precision and decrease the response

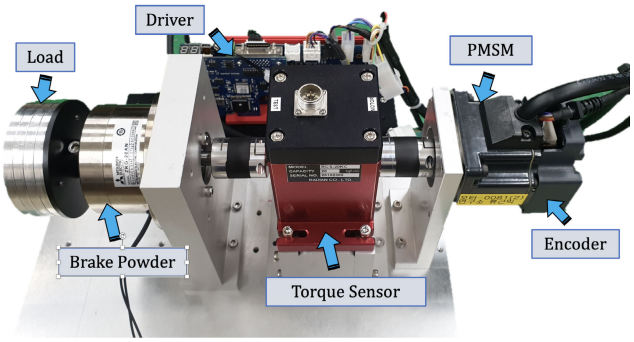

FIGURE 5. Experimental system.

time and overshoot, compared to conventional speed controllers. To control the speed of the PMSM, the difference between the desired angular speed and the actual angular speed is used as the state variables in the control system. The error of speed can be expressed as

$$e_\omega = \omega_m^{ref} - \omega_m \tag{29}$$

where the reference motor speed is designated as ω_m^{ref} and the actual feedback motor speed is represented by ω_m.

With the estimated mechanical parameters, the state space equation for the speed control system can be derived from the motor motion equation in (5) and (29).

$$\dot{e}_\omega = \dot{\omega}_m^{ref} - \frac{K_t i_Q}{\hat{J}_r} + \frac{\hat{B}_r \omega_m}{\hat{J}_r} + \frac{\hat{T}_L}{\hat{J}_r} \tag{30}$$

The sliding mode controller uses a specific reaching law and sliding surface to ensure that the equilibrium point is reached within a finite amount of time. There are two kinds of common-reaching laws (RL) as follows:

$$\begin{cases} RL_1 \rightarrow \dot{S} = -\varepsilon_\omega sgn\,(S) - q_\omega S \\ RL_2 \rightarrow \dot{S} = -\varepsilon_\omega\,|S|^a\,sgn\,(S) \end{cases} \tag{31}$$

where, ε_ω and q_ω are positive constants, and the exponential term $q_\omega S$ can enhance the system's approach to the sliding mode with the value of S. This results in a faster convergence rate compared to the conventional reaching law of $\dot{S} = -\varepsilon_\omega sgn\,(S)$. Additionally, RL_2 uses the term $|S|^a$ to decrease overshoot by adjusting the value when the state is far away from the sliding mode. In this study, a combination of reaching laws RL_1 and RL_2 is utilized by taking advantage of both. The resulting equation is presented below

$$\dot{S} = -\varepsilon_\omega\,|S|^a\,sgn\,(S) - q_\omega S \tag{32}$$

This equation guarantees a faster convergence speed by the exponential term and reduces the overshoot. With the modified reaching law, the global integral sliding surface is applied in the speed controller. The sliding surface is proposed as

$$S = K_P e_\omega + K_I \int_0^t e_\omega dt + K(t) \tag{33}$$

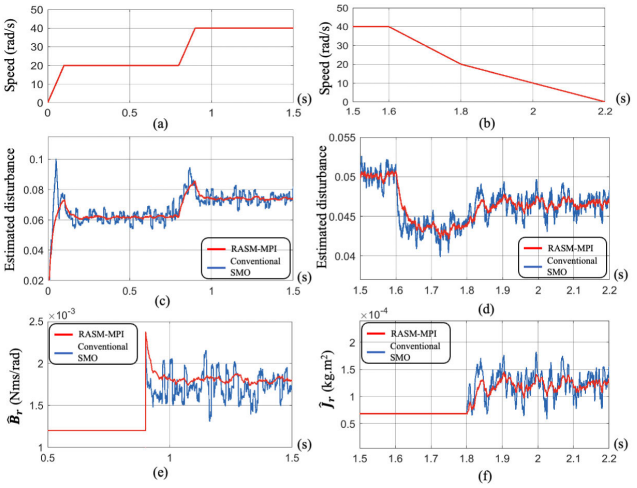

FIGURE 6. Simulation and comparison results of the estimated of $\hat{B}_r$ and $\hat{J}_r$ under setting $B_r = 1.5\,B_n, J_r = 2J_n$, and $T_L = 0.1N.m/A$. (a) and (b) Reference speed. (c) and (d) Estimated disturbance. (e) Estimated $\hat{B}_r$. (f) Estimated $\hat{J}_r$.

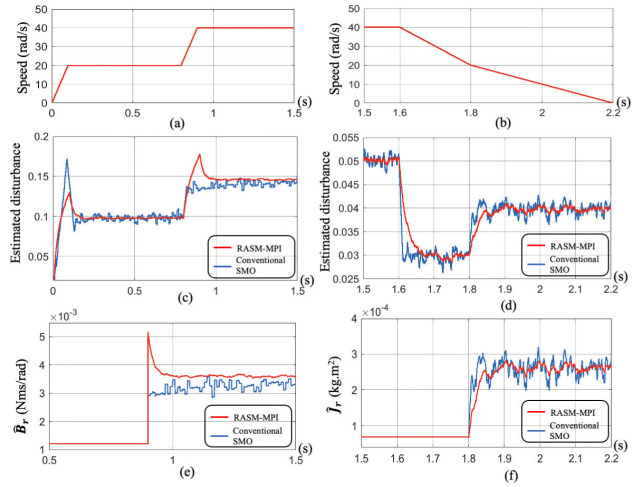

FIGURE 7. Simulation and comparison results of the estimated of $\hat{B}_r$ and $\hat{J}_r$ under setting $B_r = 3B_n, J_r = 4J_n$, and $T_L = 0.1N.m/A$. (a) and (b) Reference speed. (c) and (d) Estimated disturbance. (e) Estimated $\hat{B}_r$. (f) Estimated $\hat{J}_r$.

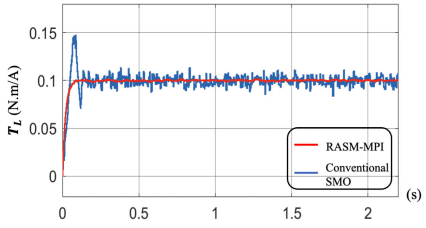

FIGURE 8. Simulation results of the estimated T_L under the RASM-MPI and SMO methods.

where K_P, K_I are positive parameters; $K(t) = \lambda_\omega e^{-a_\omega t}$ and $a_\omega > 0$ is the control input. These parameters are evaluated as stable similarly to (7).

To design an adaptive sliding-mode controller based on the integral sliding surface, the PMSM speed controller of the

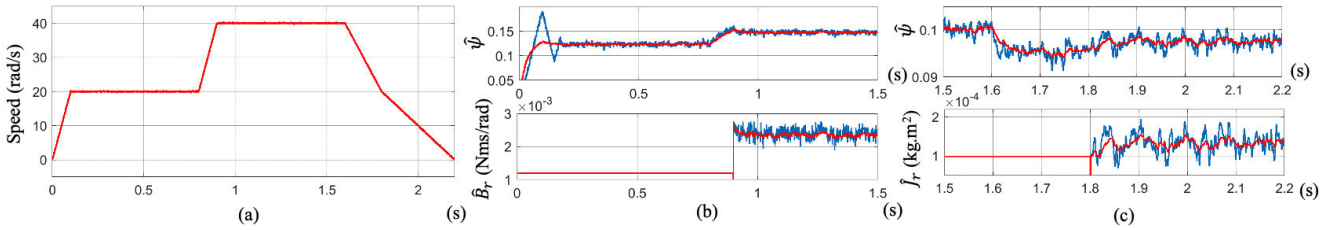

FIGURE 9. Experimental results when estimating $\hat{B}_r$ and $\hat{J}_r$. (a) Reference speed waveform. (b) Estimated $\hat{B}_r$. (c) Estimated $\hat{J}_r$.

q-axis reference current can be obtained by combining (29), (30), (32), and (33) as described below

$$\dot{S} = K_P \dot{e}_\omega + K_I e_\omega - a_\omega \lambda_\omega e^{-a_\omega t} \tag{34}$$

The equivalent control law can be obtained as

$$i_Q = \frac{\hat{J}_r}{K_I K_P}\left[K_P\left(\dot{\omega}_m^{ref} + \frac{\hat{B}_r \omega_m}{\hat{J}_r} + \frac{\hat{T}_L}{\hat{J}_r}\right) + K_I e_\omega - a_\omega K(t)\right] + \varepsilon_\omega |S|^a \, sgn(S) + q_\omega S \tag{35}$$

The stability conditions for the adaptive sliding-mode controller have been analyzed using a Lyapunov function $V(x) = s^2/2$. The reachability analysis indicates that if the system is stable, then

$$\dot{V}(x) = S\dot{S} < 0 \tag{36}$$

$$\dot{V}(x) = S\dot{S} = S\left(-\varepsilon_\omega |S|^a \, sgn(S) - q_\omega S\right) = -\varepsilon_\omega |S|^a |S| - q_\omega S^2 \tag{37}$$

As ε_ω and q_ω are positive constants in equation (37) resulting in a negative value for $\dot{V}$. This indicates that the Lyapunov function is decreasing over time, implying the stability of the system. Hence, through the application of Lyapunov's theory, the speed error in (29) can be made to converge to zero within a finite time frame by properly designing the sliding surface described in (33) and the sliding mode control law specified in (32). Fig. 4 shows the ASMSC structure of the PMSM system based on the proposed algorithm. The effectiveness of the proposed observer and controller is demonstrated through comparison with traditional techniques, both in simulations and actual experiments.

V. SIMULATION AND EXPERIMENTAL RESULTS

In this section, a simulation and an experimental system for PMSM speed control were built to assess the performance of the proposed parameter estimation approach. The simulation was conducted using MATLAB/Simulink, while the experimental system consisted of a PMSM model connected to an optical encoder (Fastech Co., K6LS30N2 motor model) and controlled by an MCU STM32F446VCT6, as shown in Fig. 5. The PMSM is connected to an incremental encoder with 20000 pulses per rev. To evaluate the disturbance rejection performance, a powder clutch (Mitsubishi Co., ZKG20AN model) was attached to the motor shaft to generate external load torque T_L. The current control loop operates at a sampling frequency of $20kHz$ and the speed and position controller operates at a $2kHz$ frequency. The current is measured with a 12-bit ADC. Table 1 lists the parameters of the PMSM used in the experiment. The RASM-MPI parameters are a constant switching gain $\varepsilon = -2$, sliding mode parameter $m = -20$, positive coefficients of the sliding mode surface $k_p = 20$, and $k_i = 500$. The ASMSC parameters are positive constant gains $\varepsilon_\omega = q_\omega = 1$, and positive coefficients of the sliding mode surface $K_P = 10$, and $K_I = 5$. These gains are selected based on the stability analysis of the sliding mode system from (16), (37), and the Heuristic tuning method.

Fig. 6 and Fig. 7 show the results of simulations that estimate the parameters $\hat{B}_r$ and $\hat{J}_r$ under various ratios. According to the results, both the newly proposed method and the conventional sliding mode observer method have the ability to estimate the $\hat{B}_r$ parameter the system is operating at two different speeds ($20rad/s \approx 190rpm$, and $40rad/s \approx 380rpm$). After updating the B_r parameter, the estimation of $\hat{J}_r$ takes place when the system goes through a state of deceleration.

In Fig. 6, the parameters are configured as $B_r = 1.5\,B_n = 1.8 \times 10^{-3} N.m.s/rad$, $J_r = 2J_n = 1.37 \times 10^{-4} kg.m^2$, and $T_L = 0.1N.m/A$. The reference speed waveform is presented in Fig. 6(a)(b). The compensation of the estimated disturbance, represented as $\hat{\psi}$, is shown in Fig. 6(c)(d) for both the conventional sliding mode observer method and the proposed method.

The proposed method (RASM-MPI) has lower and more consistent disturbance errors, leading to more precise results. As shown in Fig. 6(e), the estimated value of $\hat{B}_r$ using the proposed method is around $1.784 \times 10^{-3} N.m.s/rad$ with an error of less than 0.8%, whereas the conventional method has an error of about 5%. In addition to Fig. 6(f), the proposed method has a $\hat{J}_r$ estimation error of less than 1%, compared to the larger 8% error of the conventional method. In Fig. 7, the parameters are set as $B_r = 3B_n = 3.6 \times 10^{-3} N.m.s/rad$, $J_r = 4J_n = 2.74 \times 10^{-4} kg.m^2$, and $T_L = 0.1N.m/A$, with the reference speed waveform shown in Fig. 7(a) and (b). In Fig. 7(e), the estimated value of $\hat{B}_r$ using the proposed method is around $3.58 \times 10^{-3} N.m.s/rad$ with an error of less than 0.5%, whereas the conventional method has an error of about 11%. In addition to Fig. 7(f), the proposed method has a $\hat{J}_r$ estimation error of less than 0.9%, compared to the larger 6% error of the conventional method. Fig. 8 illustrates

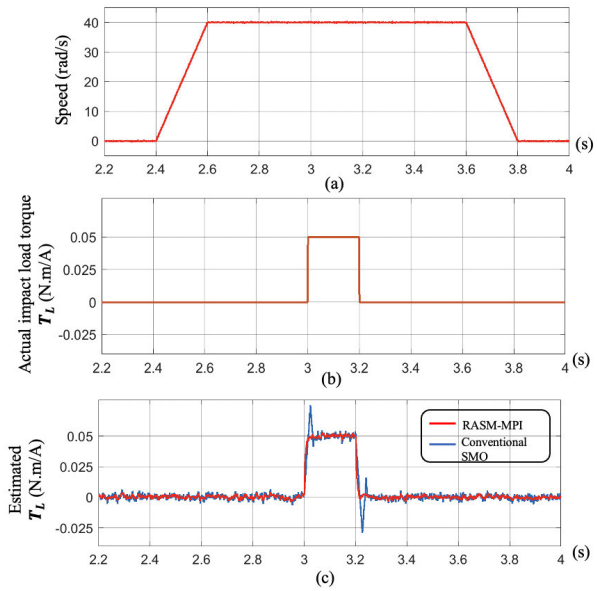

FIGURE 10. Experimental results of estimated T_L when applying the sudden load torque under the RASM-MPI and SMO methods. (a) Reference speed. (b) Load Torque is generated by the brake. (c) Estimated T_L.

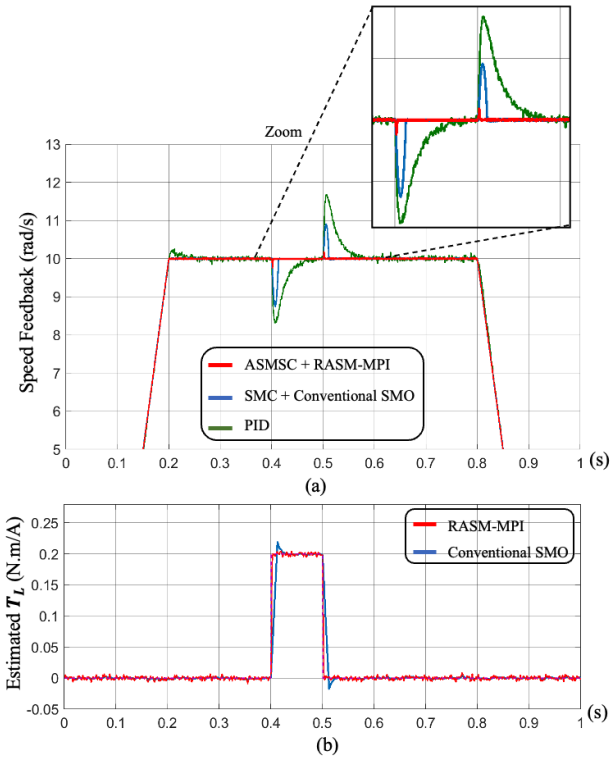

FIGURE 11. Experimental results of the speed performance response with $\omega_m^{ref} = 10rad/s \approx 95r/min$ and $T_L = 0.2N.m/A$ under the three methods: PID, SMC+SMO, and ASMSC+RASM-MPI. (a) Speed feedback. (b) Estimated T_L.

the estimated load torque for both methods after updating B_r and J_r. It is worth mentioning that the proposed method can precisely, efficiently, and stably estimate load torque,

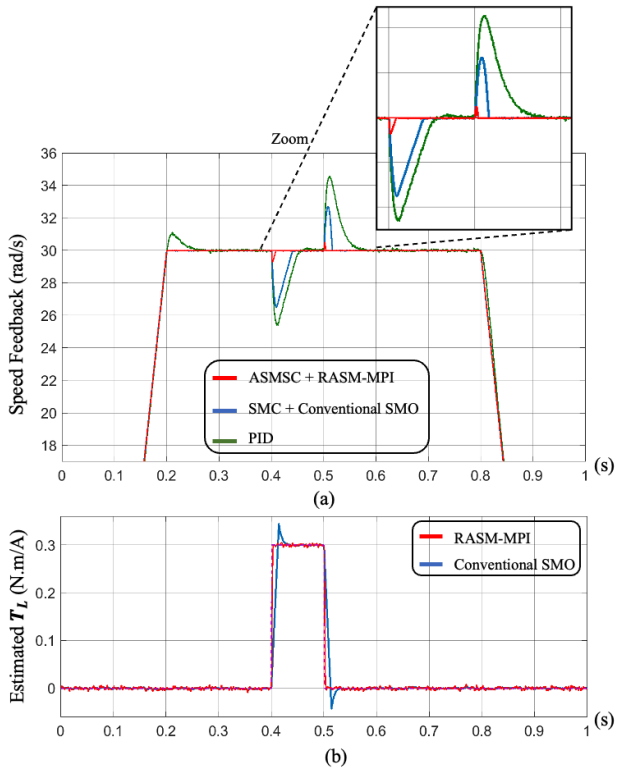

FIGURE 12. Experimental results of the speed performance response with $\omega_m^{ref} = 30rad/s \approx 285r/min$ and $T_L = 0.3N.m/A$ under the three methods: PID, SMC+SMO, and ASMSC+RASM-MPI. (a) Speed feedback. (b) Estimated T_L.

making it useful for compensating for sudden load torque and disturbance torque in real time.

Fig. 9 shows the parameter estimation experiment. Fig. 9(b) and (c) compare the estimated results of the proposed method (red line) and the conventional SMO (blue line). The RASM-MPI can reduce chattering and obtain a faster reaching time than the SMO. After the first rotation to estimate B_r and J_r, a second rotation using the speed waveform shown in Fig. 10(a) is performed to evaluate the estimated load torque. At $t = 3s$, a sudden load torque is generated by the powder clutch of about 0.05 $N.m/A$. The estimated load torque with conventional SMO has an overshoot of 40% when the load changes suddenly and vibrations occur during the estimation process. Meanwhile, method RASM-MPI gives accurate results and quickly converges to the actual value, as shown in Fig. 10(c).

To prove the effect of RASM-MPI on the speed controller, the experiment results use the estimated load torque to compensate for the sudden load torque and disturbance load torque. Moreover, Fig. 11 and Fig. 12 compare the results of three different control methods (PID, SMC+SMO, and ASMSC+RASM-MPI). The performance of the speed feedback is compared in Fig. 11(a) when the reference speed is $10rad/s \approx 95r/min$. The speed feedback of the PI control has an overshoot of about 2% at $t = 0.2$, while the methods SMC+SMO and ASMSC+RASM-MPI

have overshoots of less than 0.5%. To test their ability to compensate for suddenly changing load torque, a load torque of $T_L = 0.2N.m/A$ is generated by controlling the brake at time $t = 0.4$. The dynamic response of the system with the ASMSC+RASM-MPI method is better than the PID and SMC+SMO methods. Moreover, the proposed method ASMSC+RASM-MPI demonstrates better disturbance rejection performance compared to PID and SMC+SMO. Even when the speed and sudden load torque are set to a higher level ($30rad/s \approx 285r/min$ and $T_L = 0.3N.m/A$) in Fig. 12, the ASMSC+RASM-MPI still provides the best speed performance with accurate load torque estimation, with an overshoot speed less than 0.5% and quick responsiveness to changes in the load torque. These results indicate that the ASMSC+RASM-MPI method offers improved dynamic responses compared to PID and the conventional SMC+SMO methods.

VI. CONCLUSION

In this research, a new technique is proposed to enhance the accuracy of the PMSM system's mechanical parameter estimation and speed response. The proposed method is a combination of RASM-MPI and ASMSC, which leverages the RASM-MPI's ability to reduce chattering and accurately estimate parameters and the ASMSC's ability to mitigate overshoot and speed up convergence during sudden changes in load torque. The effectiveness of the ASMSC+RASM-MPI has been validated through simulation and experimental results, which illustrate that the proposed method obtains a better dynamic response than the SMC+SMO and PID. The method not only achieves accurate parameter estimation in a short time, while greatly improving the speed operation accuracy.

REFERENCES

[1] A. Athavale, K. Sasaki, B. S. Gagas, T. Kato, and R. D. Lorenz, "Variable flux permanent magnet synchronous machine (VF-PMSM) design methodologies to meet electric vehicle traction requirements with reduced losses," *IEEE Trans. Ind. Appl.*, vol. 53, no. 5, pp. 4318–4326, Sep. 2017.

[2] P. Niazi, H. A. Toliyat, and A. Goodarzi, "Robust maximum torque per ampere (MTPA) control of PM-assisted SynRM for traction applications," *IEEE Trans. Veh. Technol.*, vol. 56, no. 4, pp. 1538–1545, Jul. 2007.

[3] T. H. Nguyen and D. Lee, "Deterioration monitoring of DC-link capacitors in AC machine drives by current injection," *IEEE Trans. Power Electron.*, vol. 30, no. 3, pp. 1126–1130, Mar. 2015.

[4] Y. He, Y. Wang, Y. Feng, and Z. Wang, "Parameter identification of an induction machine at standstill using the vector constructing method," *IEEE Trans. Power Electron.*, vol. 27, no. 2, pp. 905–915, Feb. 2012.

[5] N. Hoffmann and F. W. Fuchs, "Minimal invasive equivalent grid impedance estimation in inductive-resistive power networks using extended Kalman filter," *IEEE Trans. Power Electron.*, vol. 29, no. 2, pp. 631–641, Feb. 2014.

[6] H. Renaudineau, J. Martin, B. Nahid-Mobarakeh, and S. Pierfederici, "DC–DC converters dynamic modeling with state observer-based parameter estimation," *IEEE Trans. Power Electron.*, vol. 30, no. 6, pp. 3356–3363, Jun. 2015.

[7] Y. Feng, X. Yu, and F. Han, "High-order terminal sliding-mode observer for parameter estimation of a permanent-magnet synchronous motor," *IEEE Trans. Ind. Electron.*, vol. 60, no. 10, pp. 4272–4280, Oct. 2013.

[8] K. Fujita and K. Sado, "Instantaneous speed detection with parameter identification for AC servo system," *IEEE Trans. Ind. Appl.*, vol. 28, no. 4, pp. 864–872, Jul./Aug. 1992.

[9] I. Awaya, Y. Kato, I. Miyake, and M. Ito, "New motion control with inertia identification function using disturbance observer," in *Proc. Int. Conf. Ind. Electron., Control, Instrum., Autom.*, 1992, pp. 77–81.

[10] J.-W. Choi, S.-C. Lee, and H.-G. Kim, "Inertia identification algorithm for high-performance speed control of electric motors," *IEE Proc.-Electr. Power Appl.*, vol. 153, no. 3, pp. 379–386, May 2006.

[11] S.-M. Yang and Y.-J. Deng, "Observer-based inertial identification for auto-tuning servo motor drives," in *Proc. 14th IAS Annu. Meeting, Conf. Rec. Ind. Appl. Conf.*, Hong Kong, Oct. 2005, pp. 968–972.

[12] X. Zhang and Z. Li, "Sliding-mode observer-based mechanical parameter estimation for permanent magnet synchronous motor," *IEEE Trans. Power Electron.*, vol. 31, no. 8, pp. 5732–5745, Aug. 2016.

[13] J. Davila, L. Fridman, and A. Poznyak, "Observation and identification of mechanical systems via second order sliding modes," *Int. J. Control*, vol. 79, no. 10, pp. 1251–1262, Oct. 2006.

[14] J. Davila, L. Fridman, and A. Levant, "Second-order sliding-mode observer for mechanical systems," *IEEE Trans. Autom. Control*, vol. 50, no. 11, pp. 1785–1789, Nov. 2005.

[15] S. Yang and K. Lin, "Automatic control loop tuning for permanent-magnet AC servo motor drives," *IEEE Trans. Ind. Electron.*, vol. 63, no. 3, pp. 1499–1506, Mar. 2016.

[16] L. Sheng, G. Xiaojie, and Z. Lanyong, "Robust adaptive backstepping sliding mode control for six-phase permanent magnet synchronous motor using recurrent wavelet fuzzy neural network," *IEEE Access*, vol. 5, pp. 14502–14515, 2017.

[17] H. Tran Ngoc, T. T. Nguyen, H. Q. Cao, K. M. Le, and J. W. Jeon, "Improving the accuracy of permanent magnet rotor position estimation for stepper motors using magnetic induction and harmonic rejection," *IET Power Electron.*, vol. 13, no. 11, pp. 2236–2244, Aug. 2020.

[18] M. Masiala, B. Vafakhah, J. Salmon, and A. M. Knight, "Fuzzyself-tuning speed control of an indirect field-oriented control induction motor drive," *IEEE Trans. Ind. Appl.*, vol. 44, no. 6, pp. 1732–1740, Nov./Dec. 2008.

[19] H. H. Choi and J. Jung, "Discrete-time fuzzy speed regulator design for PM synchronous motor," *IEEE Trans. Ind. Electron.*, vol. 60, no. 2, pp. 600–607, Feb. 2013.

[20] T. Tarczewski and L. M. Grzesiak, "Constrained state feedback speed control of PMSM based on model predictive approach," *IEEE Trans. Ind. Electron.*, vol. 63, no. 6, pp. 3867–3875, Jun. 2016.

[21] M. Preindl and S. Bolognani, "Model predictive direct speed control with finite control set of PMSM drive systems," *IEEE Trans. Power Electron.*, vol. 28, no. 2, pp. 1007–1015, Feb. 2013.

[22] Y. Yi, D. M. Vilathgamuwa, and M. A. Rahman, "Implementation of an artificial-neural-network-based real-time adaptive controller for an interior permanent-magnet motor drive," *IEEE Trans. Ind. Appl.*, vol. 39, no. 1, pp. 96–104, Jan. 2003.

[23] H. N. Tran, K. M. Le, and J. W. Jeon, "Adaptive current controller based on neural network and double phase compensator for a stepper motor," *IEEE Trans. Power Electron.*, vol. 34, no. 8, pp. 8092–8103, Aug. 2019.

[24] A. Wang, X. Jia, and S. Dong, "A new exponential reaching law of sliding mode control to improve performance of permanent magnet synchronous motor," *IEEE Trans. Magn.*, vol. 49, no. 5, pp. 2409–2412, May 2013.

[25] X. Yu and O. Kaynak, "Sliding-mode control with soft computing: A survey," *IEEE Trans. Ind. Electron.*, vol. 56, no. 9, pp. 3275–3285, Sep. 2009.

[26] T. H. Nguyen, T. T. Nguyen, V. Q. Nguyen, K. M. Le, H. N. Tran, and J. W. Jeon, "An adaptive sliding-mode controller with a modified reduced-order proportional integral observer for speed regulation of a permanent magnet synchronous motor," *IEEE Trans. Ind. Electron.*, vol. 69, no. 7, pp. 7181–7191, Jul. 2022.

[27] T. H. Nguyen, T. T. Nguyen, H. N. Tran, and J. W. Jeon, "An improved sliding mode control using reduced-order PI observer for PMSM system," in *Proc. 16th Int. Conf. Ubiquitous Inf. Manage. Commun. (IMCOM)*, Jan. 2022, pp. 1–5.

[28] T. H. Nguyen, T. T. Nguyen, K. Minh Le, H. N. Tran, and J. W. Jeon, "An adaptive backstepping sliding-mode control for improving position tracking of a permanent-magnet synchronous motor with a nonlinear disturbance observer," *IEEE Access*, vol. 11, pp. 19173–19185, 2023.

[29] T. Li, X. Liu, and H. Yu, "Backstepping nonsingular terminal sliding mode control for PMSM with finite-time disturbance observer," *IEEE Access*, vol. 9, pp. 135496–135507, 2021.

[30] M. Lazor and M. Stulrajter, "Modified field oriented control for smooth torque operation of a BLDC motor," in *Proc. ELEKTRO*, May 2014, pp. 180–185.

[31] H. N. Tran, T. T. Nguyen, T. H. Nguyen, B. V. Nguyen, H. Q. Cao, and J. W. Jeon, "Online-tuning of speed and position controllers using particle swarm optimization algorithm for a BLDC motor," in *Proc. 16th Int. Conf. Ubiquitous Inf. Manag. Commun. (IMCOM)*, Jan. 2022, pp. 1–7.
[32] H. N. Tran, T. T. Nguyen, H. Q. Cao, T. H. Nguyen, H. X. Nguyen, and J. W. Jeon, "Auto-tuning controller using MLPSO with K-means clustering and adaptive learning strategy for PMSM drives," *IEEE Access*, vol. 10, pp. 18820–18831, 2022.
[33] T. T. Nguyen, H. N. Tran, T. H. Nguyen, and J. W. Jeon, "Recurrent neural network-based robust adaptive model predictive speed control for PMSM with parameter mismatch," *IEEE Trans. Ind. Electron.*, vol. 70, no. 6, pp. 6219–6228, Jun. 2023.
[34] F. M. Zaihidee, S. Mekhilef, and M. Mubin, "Robust speed control of PMSM using sliding mode control (SMC)—A review," *Energies*, vol. 12, no. 9, p. 1669, May 2019.

HOANG NGOC TRAN received the B.S. degree in mechatronics engineering from the Ho Chi Minh City University of Technology, Ho Chi Minh City, Vietnam, in 2015, and the Ph.D. degree in electrical and computer engineering from Sungkyunkwan University, Suwon, South Korea, in 2020. From 2020 to 2022, he was a Postdoctoral Researcher with the Department of Electrical and Computer Engineering, Sungkyunkwan University. Since 2022, he has been a Lecturer and a Researcher with the Department of Software Engineering, FPT University, Can Tho, Vietnam. His research interests include signal processing, motion control, embedded systems, autonomous robotics, and machine learning.

JAE WOOK JEON (Senior Member, IEEE) received the B.S. and M.S. degrees in electronics engineering from Seoul National University, Seoul, South Korea, in 1984 and 1986, respectively, and the Ph.D. degree in electrical engineering from Purdue University, West Lafayette, IN, USA, in 1990.

From 1990 to 1994, he was a Senior Researcher with Samsung Electronics, Suwon, South Korea. Since 1994, he has been with Sungkyunkwan University, Suwon, where he was first an Assistant Professor with the School of Electrical and Computer Engineering and is currently a Professor with the School of Information and Communication Engineering. His research interests include robotics, embedded systems, and factory automation.